Citation: Molecular Therapy — Oncolytics (2015) **1,** 14010; doi:10.1038/mto.2014.10

www.nature.com/mto

ARTICLE

Oncolytic HSV virotherapy in murine sarcomas differentially triggers an antitumor T-cell response in the absence of virus permissivity

Jennifer L Leddon[1,2,3], Chun-Yu Chen[1], Mark A Currier[1], Pin-Yi Wang[1], Francesca A Jung[1], Nicholas L Denton[1], Kevin M Cripe[1], Kellie B Haworth[1,4], Michael A Arnold[5], Amy C Gross[6], Timothy D Eubank[6], William F Goins[7], Joseph C Glorioso[7], Justus B Cohen[7], Paola Grandi[7], David A Hildeman[8] and Timothy P Cripe[1,4]

Multiple studies have indicated that in addition to direct oncolysis, virotherapy promotes an antitumor cytotoxic T cell response important for efficacy. To study this phenomenon further, we tested three syngeneic murine sarcoma models that displayed varied degrees of permissiveness to oncolytic herpes simplex virus replication and cytotoxicity *in vitro*, with the most permissive being comparable to some human sarcoma tumor lines. The *in vivo* antitumor effect ranged from no or modest response to complete tumor regression and protection from tumor rechallenge. The *in vitro* permissiveness to viral oncolysis was not predictive of the *in vivo* antitumor effect, as all three tumors showed intact interferon signaling and minimal permissiveness to virus *in vivo*. Tumor shrinkage was T-cell mediated with a tumor-specific antigen response required for maximal antitumor activity. Further analysis of the innate and adaptive immune microenvironment revealed potential correlates of susceptibility and resistance, including favorable and unfavorable cytokine profiles, differential composition of intratumoral myeloid cells, and baseline differences in tumor cell immunogenicity and tumor-infiltrating T-cell subsets. It is likely that a more complete understanding of the interplay between the immunologic immune microenvironment and virus infection will be necessary to fully leverage the antitumor effects of this therapeutic platform.

Molecular Therapy — Oncolytics (2015) **1**, 14010; doi:10.1038/mto.2014.10; published online 21 January 2015

INTRODUCTION

Over 15,000 children are newly diagnosed with cancer in the United States each year.[1] While progressive advances have steadily improved survival for some pediatric tumor types, progress for pediatric sarcomas has essentially stalled over the past two decades.[2] Although some localized tumors are sensitive to standard therapies, including surgical resection, radiation, and chemotherapy, relapse and metastasis are common and are often chemoresistant. Despite aggressive multimodal therapy, cure rates for patients with relapsed or metastatic sarcoma remain less than 30%. Therefore, there remains a significant need for novel sarcoma therapies both to improve local control and to treat metastatic disease.

The development of attenuated, oncolytic herpes simplex virus (oHSV) mutants engineered to achieve tumor-selective virus replication is being actively pursued by many investigators and pharmaceutical companies.[3–6] Early-phase clinical trials have reported safety of administering attenuated oHSV mutants to humans by intracranial,[7,8] intralesional,[9] and hepatic artery routes.[10] Recent data reported by Amgen for T-Vec, an HSV-1 mutant engineered to express granulocyte-macrophage colony-stimulating factor (GM-CSF), are encouraging with 16.3% of melanoma patients exhibiting a durable response, compared with 2% of patients in the control arm using GM-CSF alone without virus.[11]

Classically, the mechanism of cell death induced by oncolytic virotherapy is thought to be direct infection of tumor cells with virus replication leading to cell lysis, virus amplification, and spread to neighboring tumor cells, driving significant efforts in the field toward improving viral kinetics. However, emerging data suggest that oHSV exerts an antitumor effect through multiple distinct mechanisms including stimulation of antitumor T-cell immunity. Data from the Amgen trial suggest that T-cell–dependent mechanisms of oHSV efficacy are operative in immunocompetent patients and likely contribute to the eradication of both local tumors and distant metastases.[11,12]

[1]Center for Childhood Cancer and Blood Diseases, Nationwide Children's Hospital, The Ohio State University, Columbus, Ohio, USA; [2]Medical Scientist Training Program, Cincinnati Children's Hospital Medical Center, University of Cincinnati, Cincinnati, Ohio, USA; [3]Immunobiology Graduate Training Program, Cincinnati Children's Hospital Medical Center, University of Cincinnati, Cincinnati, Ohio, USA; [4]Division of Hematology/Oncology/Blood and Marrow Transplantation, Nationwide Children's Hospital, The Ohio State University, Columbus, Ohio, USA; [5]Department of Pathology and Laboratory Medicine, Nationwide Children's Hospital, The Ohio State University, Columbus, Ohio, USA; [6]Division of Pulmonary, Allergy, Critical Care & Sleep Medicine, The Ohio State University, Columbus, Ohio, USA; [7]Department of Microbiology and Molecular Genetics, University of Pittsburgh, School of Medicine, Pittsburgh, Pennsylvania, USA; [8]Division of Cellular and Molecular Immunology, Cincinnati Children's Hospital Medical Center, University of Cincinnati, Cincinnati, Ohio, USA. Correspondence: Timothy P Cripe (timothy.cripe@nationwidechildrens.org)
Received 7 July 2014; accepted 14 October 2014

Although such T-cell–dependent effects of oHSV virotherapy have been demonstrated in multiple mouse tumor models, much published preclinical data have used human tumor xenografts in immunodeficient mice, largely driven by the perceived poor permissivity of murine tumors to infection with human HSV-1. To date, determination of the relative contribution of T-cells to the efficacy of oHSV in pediatric sarcomas has been limited by the paucity of immunocompetent tumor models. Recent advances in elucidating the molecular pathways that drive rhabdomyosarcomagenesis have led to the development of multiple immunocompetent mouse models of rhabdomyosarcoma (RMS) that recapitulate many aspects of rhabdomyosarcoma biology and histology.[13,14]

We have previously reported that human rhabdomyosarcoma cell lines and xenograft models are sensitive to oHSV virotherapy.[15,16] To more accurately assess the role of the immune response to virus, we thus acquired and tested several diverse transplantable mouse sarcoma models in their native C57Bl/6 strain background. These studies are the first evaluation of oHSV efficacy in immunocompetent pediatric sarcoma models and provide a robust *in vitro* comparison of available mouse lines to their human counterparts including viral receptor expression, susceptibility to infection (virus entry), and permissiveness to oHSV replication.

RESULTS

Virus entry

As an initial assessment of HSV-1 receptor expression, we queried an Affymetrix database of 95 pediatric tumor cell lines in the Pediatric Preclinical Testing Program (http://pptp.nchresearch.org) for expression levels of the major HSV-1 receptors. Human RMS cell lines expressed high levels of *Nectin-1*, relative to other pediatric tumor types, and displayed minimal expression of other HSV-entry receptors, *Nectin-2* and *herpesvirus entry mediator (HVEM*; Figure 1a). Affymetrix expression data were confirmed in four cell lines by quantitative reverse transcription polymerase chain reaction (qRT-PCR) (data not shown) and flow cytometric analyses (Figure 1b).

We tested two previously established cell line models of mouse RMS, 76-9 (methylchloranthrene-induced) and M3-9-M ($p53^{-/-}$ and transgenic for hepatocyte growth factor/scatter factor (*HGF/SF*)),[17,18] and HGF116, which we derived from a spontaneous neck mass in a female HGF/SF_{tg}, $INK4a/Arf^{-/-}$ mouse, previously reported to

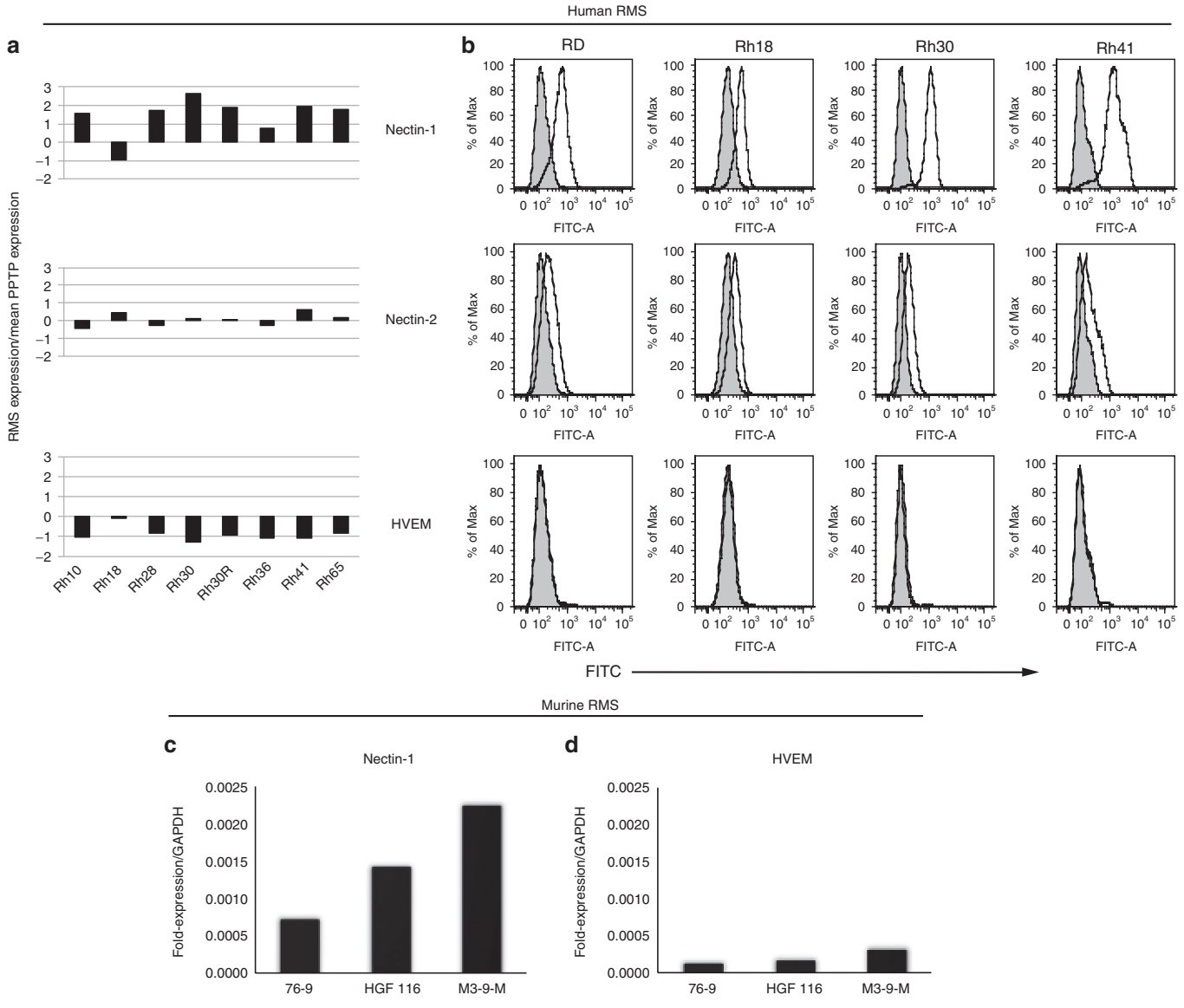

promote rhabdomyosarcomagenesis.[19] HGF116 has a histological phenotype consistent with sarcoma and expresses the human RMS markers Myogenin and MyoD (data not shown).

We first analyzed these cell lines for the expression of HSV-1 entry receptors to determine if low expression is a significant barrier to the utility of these models for the study of oncolytic HSV virotherapy. Similar to their human counterparts, mouse RMS tumor cell lines displayed variable expression of the major HSV entry receptor *Nectin-1*, with 76-9 and HGF116 showing levels similar to those in normal mouse spleen and M3-9-M twofold to threefold higher and ~40% of the level found in thymus (the highest of normal organs tested), with minimal expression of *HVEM* (Figure 1c and Supplementary Figure S1). We confirmed functional Nectin-1 on human and mouse cell lines by gene transfer assays using receptor-restricted HSV glycoprotein D mutant viruses,[20] whose cell specificity we previously confirmed using Chinese hamster ovary cells normally lacking HSV-1 receptors that were retrovirally transduced to express specific receptors (Supplementary Figure S1 in ref. 21; Figure 1e). Cells were infected with K26GFP (wild-type gD), or its receptor-restricted derivatives d5-28V (Nectin-1-restricted) and A3C/Y38C (HVEM-restricted). All human and mouse RMS cell lines were susceptible to wild-type HSV gene transfer, as measured by flow cytometry for green fluorescent protein (GFP) expression. In all cases, the transduction efficiency of Nectin-1–restricted virus was similar to that of wild-type HSV-1, whereas little to no transduction was seen with the HVEM-restricted virus. Thus, both human and mouse RMS cells are susceptible to HSV-mediated gene transfer and predominantly utilize the Nectin-1 receptor for viral entry.

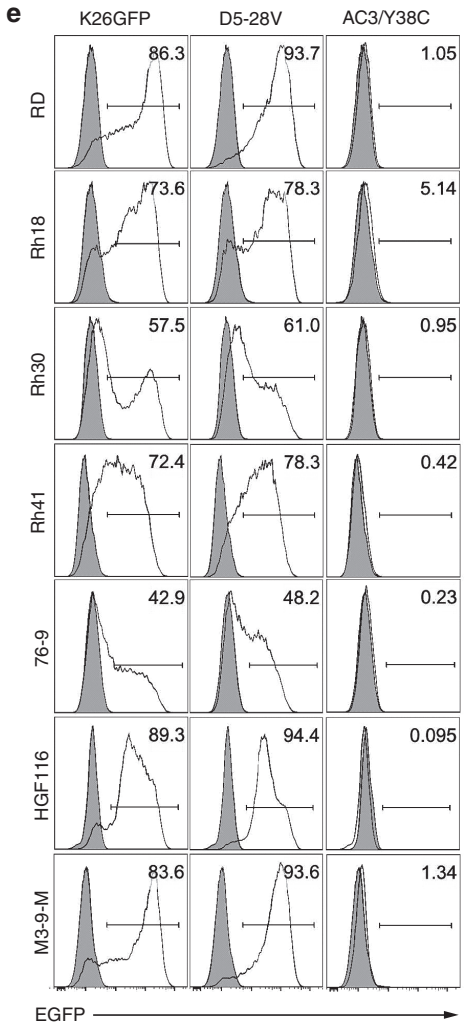

Figure 1 Human and mouse sarcoma cell lines express the major HSV entry receptor Nectin-1 and are susceptible to HSV-mediated gene transfer. (**a**) Microarray analysis of the major HSV-entry receptors Nectin-1, Nectin-2, and HVEM in eight human RMS tumor models relative to their mean expression in all pediatric tumor cell lines and xenografts in the Pediatric Preclinical Testing Program. (**b**) FACS analysis of HSV receptor expression in four human RMS models; shaded areas represent isotype control, open lines represent receptor-specific staining. Real-time qRT-PCR analysis of HSV receptor expression of (**c**) *Nectin-1* and (**d**) *HVEM* in three mouse sarcoma models. Error bars, SD ($n = 3$). (**e**) Gene transfer assay. Human and mouse sarcoma cells were infected with EGFP-expressing HSV-1, K26GFP (wild-type gD), or its receptor-restricted derivatives d5-28V (Nectin-restricted) and A3C/Y38C (HVEM-restricted).

Cell sensitivity and permissivity to oHSV

As measured by cell survival, 76-9 was highly resistant to killing by oHSV mutant rRp450 (*ICP6*$^{-/-}$) *in vitro* with a concentration inhibiting 50% growth (IC_{50}) at 4 days postinfection of greater than 10 plaque-forming units (pfu)/cell (multiplicity of infection (MOI) = 10; Figure 2a). In contrast, HGF116 and M3-9-M were susceptible to oHSV-mediated killing, with an IC_{50} for both lines of MOI ~1. The sensitivity of HGF116 and M3-9-M was similar to that of two of the human RMS lines, Rh30 and Rh41 (Figure 2b), both derived from the more aggressive alveolar type of RMS, while the IC_{50} of two embryonal type human RMS lines (RD and Rh18) was ~10-fold lower.

Consistent with its poor sensitivity to oHSV killing, 76-9 also displayed delayed viral replication kinetics; however, total viral production at 72 hours postinfection was similar for all three models (Figure 2c). A comparable delay in viral replication was observed for the two less susceptible human cell lines Rh30 and Rh41 which peaked at three logs of viral replication at 72 hours postinfection (Figure 2d). Peak viral yields were similar to those in mouse RMS models, but remained two logs below those produced by the highly susceptible embryonal type RMS lines RD and Rh18. Overall, viral replication kinetics tightly correlated with the *in vitro* killing effect, and the mouse cell lines most sensitive to cytotoxicity and the most permissive to viral replication were similar to the least sensitive and permissive human RMS cell lines.

Antitumor efficacy in immunocompetent models

Despite 76-9 being highly resistant to oHSV *in vitro*, mice bearing 76-9 tumors displayed a modestly prolonged survival following intratumoral injections of rRp450, while mice bearing HGF116 tumors showed no response to oHSV injection (Figure 3a). Further enhancement of *in vitro* HGF116 killing through overexpression of the human HSV receptor Nectin-1 failed to improve the poor *in vivo* therapeutic effect (Supplementary Figure S2). In contrast, five of eight virus-treated M3-9-M mice had a complete response with tumor shrinkage beginning at day 7 after virus injection and remained tumor free for greater than 90 days. We were unable to identify any histologic differences in cellular morphology by hematoxylin and eosin staining among the three models comparing phosphate-buffered saline (PBS)- and oHSV-treated tumors (analyzed at 1, 3, and 7 days postinfection, data not shown). The five mice with complete response and one mouse with stable disease rejected tumor rechallenge with two times the original tumor cell injection amount on the contralateral flank (Figure 3a, arrow), which stands in contrast to 5/7 (71%) age-matched control mice (tumor-naive) that developed tumors after being injected with the same cells and dose at the same time. This finding demonstrates the formation of protective antitumor immunity. Furthermore, our data

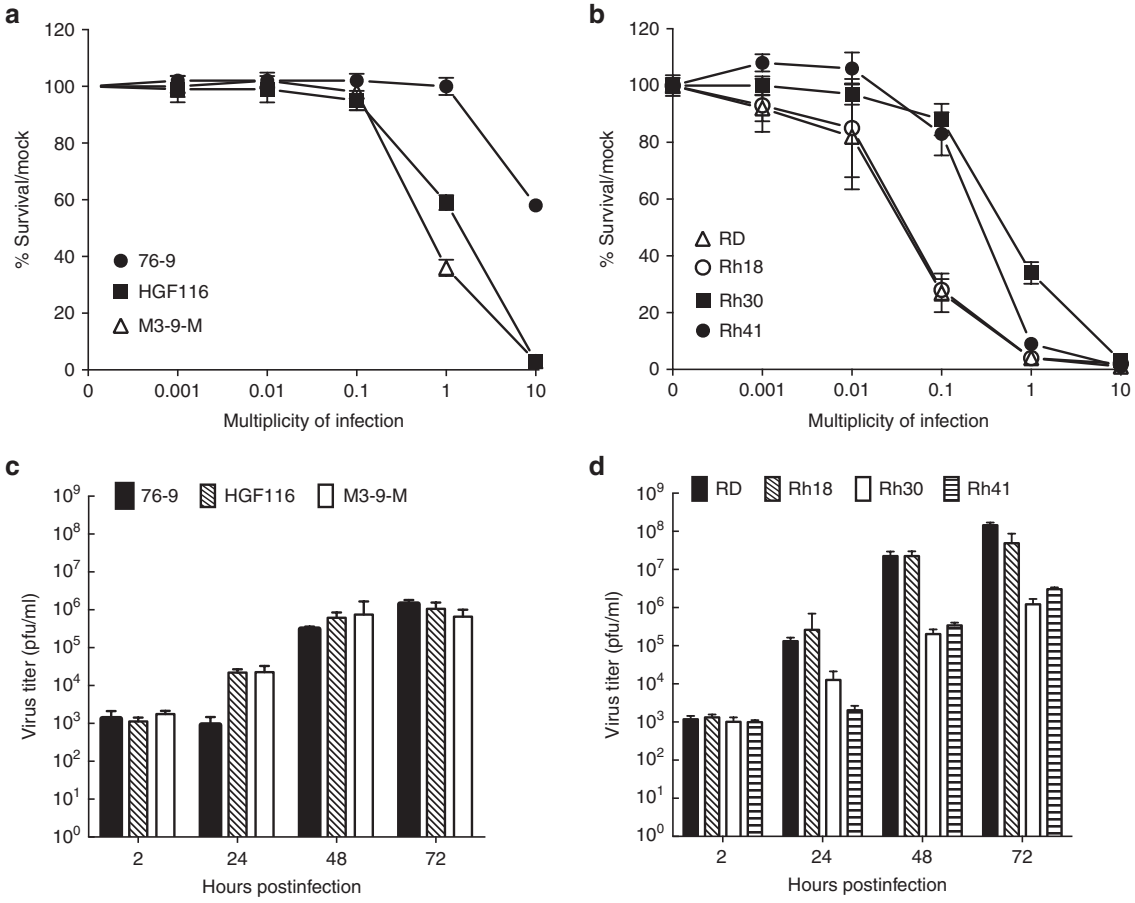

Figure 2 Human and mouse sarcoma cell lines display differential sensitivity to oHSV-mediated oncolysis and permissiveness to oHSV replication *in vitro*. (**a**) Mouse or (**b**) human RMS cells were infected with rRp450 at MOIs = 0.001, 0.01, 0.1, 1, and 10. Percent survival by MTS assay is shown relative to mock-infected control 4 days postinfection. Error bars, SEM ($n = 6$) (**c,d**) Viral replication. (**c**) Mouse or (**d**) human sarcoma cell lines were infected at MOI = 0.01, and both free and cell-associated virus were quantified by standard plaque assay at 2, 24, 48, and 72 hours postinfection. Data are shown as virus titer in the culture dishes (pfu/ml). Error bars, SEM ($n = 9$).

show a disconnection between cell autonomous sensitivity to oHSV and the observed *in vivo* antitumor effect.

Antitumor efficacy in immunodeficient models

We tested virotherapy in athymic nude mice to determine whether the therapeutic effect of oHSV in these models is T-cell dependent. In the absence of functional T-cells, 76-9 displayed no antitumor response to the same rRp450-dosing schedule that showed extended survival of syngeneic C57Bl/6 mice (Figure 3b). In contrast, the M3-9-M model, which was highly sensitive in syngeneic C57Bl/6 mice, demonstrated some antitumor efficacy in athymic nude mice. M3-9-M tumor growth was modestly delayed, and survival extended following rRp450 injection; however, we did not observe any tumor shrinkage as seen when tumors were implanted in immunocompetent C57Bl/6 mice (Figure 3b). Together, these data indicate that T cells contribute to the therapeutic effect of oHSV in immunocompetent sarcoma models and suggest that baseline differences in tumor cell immunogenicity or the virus-induced adaptive immune response may significantly influence the therapeutic outcome of oHSV *in vivo*.

Interferon responsiveness

We next tested virus production in tumors to determine if the disconnect between *in vitro* sensitivity and *in vivo* efficacy was due to differential permissivity. Although there was a modest (<0.5 log) rise in intratumoral virus titers in the two lines that were more permissive to oHSV replication *in vitro*, virus was rapidly cleared from tumors (Figure 4a). Interestingly, athymic nude mice displayed higher intratumoral viral titers in all models, which were maintained for at least 120 hours (Figure 4b). Thus, although the therapeutic effect is diminished in athymic nude mice, intratumoral virus replication is more robust and persistent.

Overall, however, intratumoral virus replication in either T-cell replete or T-cell–deficient mice was unexpectedly low, given the high permissivity of these tumor cell lines to oHSV replication *in vitro*. oHSV injection induced the expression of interferon (IFN)-stimulated genes, *MX1, PKR, PML*, and *STAT-1* in all three mouse sarcoma tumor models consistent with a type I IFN response (Figure 4c), which may play a role in restricting virus replication in these tumors. The pattern of IFN-stimulated gene stimulation in the tumors following virus injection was similar to that seen in cell lines following exposure to high levels of exogenous IFN-β (1,000 U/ml) with *Mx1* being the highest (Supplementary Figure S3), though the magnitude was far lower in the tumors. For the HGF116 and M3-9-M models, low doses of mouse IFN-β (10 U/ml) were sufficient to completely block virus replication *in vitro*, whereas 76-9 demonstrated a dose-dependent decrease in viral titers with complete inhibition at 1,000 U/ml IFN-β (Figure 4d). These data show that oHSV replication is mitigated by an intact IFN response pathway in these cells.

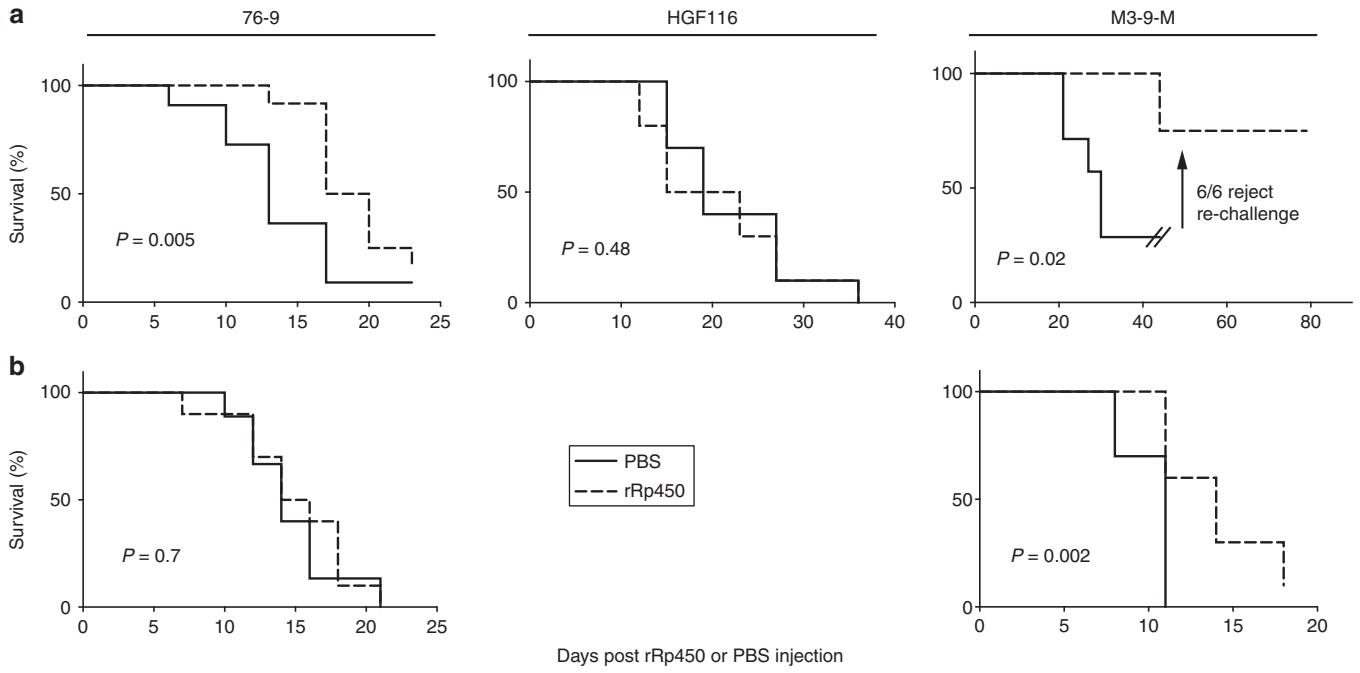

Figure 3 Mouse sarcoma models display differential antitumor responses to oncolytic HSV therapy in immunocompetent and immunodeficient mice. Mouse sarcoma cell lines, 76-9, M3-9-M, and HGF116, were implanted subcutaneously into the flanks of female (**a**) C57Bl/6 mice and (**b**) athymic nude mice. rRp450 at a dose of 1×10^8 pfu (dashed lines) or PBS control (solid lines) was delivered by fractionated intratumoral injection on days 0, 2, and 4 ($n = 8$–10). Mice were sacrificed when tumor volume reached ~2,500 mm^3, and percent survival determined by Kaplan–Meier analysis.

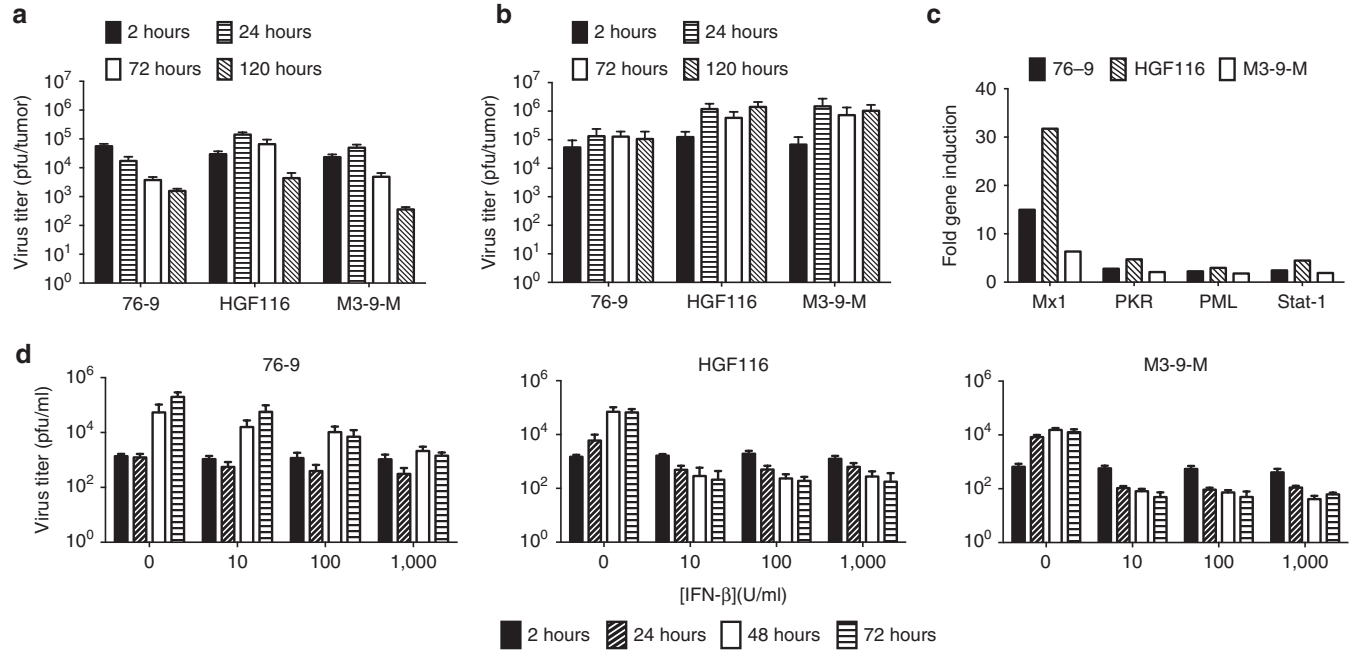

Figure 4. Mouse sarcoma models display high interferon responsiveness and minimal in vivo virus replication, which does not correlate with antitumor efficacy. Intratumoral replication of rRp450 in subcutaneous mouse sarcoma tumors implanted into female (**a**) C57Bl/6 or (**b**) athymic nude mice. Following a single injection of 1×10^7 pfu rRp450, tumors were harvested at indicated time points, homogenized, and total intratumoral virus was quantitated by plaque assay. Error bars, SEM ($n = 7$–10) (**c**) *In vivo* induction of interferon-stimulated genes (ISG) following rRp450 injection. Data shown as fold ISG gene induction over PBS-injected tumors by qRT-PCR analysis ($n = 4$–6). (**d**) Effects of exogenous IFN-β on virus replication *in vitro*. Mouse sarcoma cell lines were pretreated with varying doses of mouse IFN-β for 18 hours and then infected with MOI = 0.01 rRp450. Both free and cell-associated viruses were quantified by standard plaque assay at 2, 24, 48, and 72 hours postinfection. Error bars, SEM ($n = 9$).

Although the same effect was seen with exogenous human IFN-β in human RMS cell lines, mouse IFN-β failed to suppress virus replication in the human RMS cell lines (data not shown), consistent with known species differences. Furthermore, despite the permissiveness of murine sarcoma to oHSV replication *in vitro*, neither the magnitude of early virus replication nor persistence of virus *in vivo* correlated with differences in antitumor efficacy of oHSV virotherapy in these models.

Gender effects

Given that the therapeutic effect of oHSV in mouse RMS models is at least partially T-cell mediated, we evaluated major histocompatibility complex (MHC) class I expression among these three tumor cell lines. HGF116 and 76-9 tumor cell lines expressed very low MHC class I (Kb), which was inducible by treatment with mouse IFN-γ (Supplementary Figure S4). M3-9-M, which was highly sensitive to oHSV *in vivo*, expressed high MHC I at baseline, which was further enhanced by IFN-γ treatment. In addition to higher expression of MHC class I molecules, potentially rendering these cells more susceptible to T-cell–mediated cytolysis, M3-9-M, which was derived from a male C57Bl/6 mouse, expresses the HY antigen receptor complex (data not shown) which is a potential immunogenic target when tumors are grown in female mice. In contrast to female C57Bl/6 mice in which oHSV injection leads to dramatic tumor regression and long-term protection from rechallenge (Figure 3a), male mice, which are tolerized to HY antigen, displayed only a modest delay in tumor growth and extension of survival but no tumor reduction and no long-term survivors (Figure 5). The overall effect of oHSV therapy in M3-9-M male mice was similar to the effect observed in athymic nude mice (Figure 3b). Together, these data suggest that the dramatic tumor regression observed in female M3-9-M tumor–bearing mice may be driven by recognition of a gender-specific tumor antigen, possibly the HY antigen.

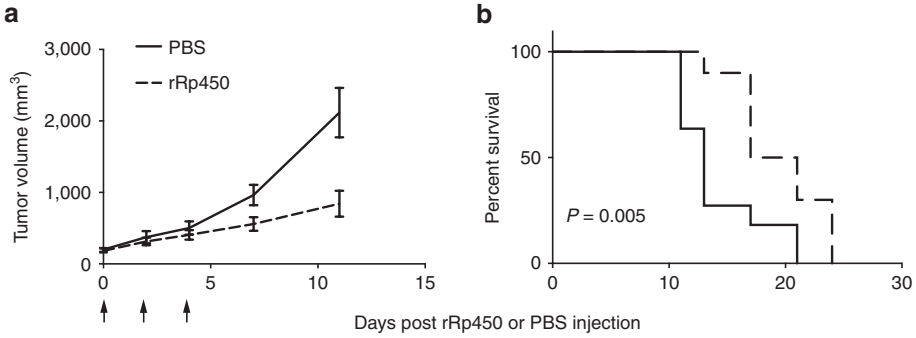

Figure 5 Sensitive model M3-9-M expresses the HY antigen and displays diminished antitumor efficacy in HY tolerant male mice. Mouse sarcoma cell lines M3-9-M was implanted subcutaneously into the flanks of male C57Bl/6 mice. rRp450 at a dose of 1×10^8 pfu (dashed lines) or PBS control (solid lines) was delivered by intratumoral injection on days 0, 2, and 4. (**a**) Average tumor volume following three doses of rRp450 or PBS. Error bars, SEM ($n = 8$–10). (**b**) Mice were sacrificed when tumor volume reached ~2,500 mm^3, and percent survival comparison determined by Kaplan–Meier analysis.

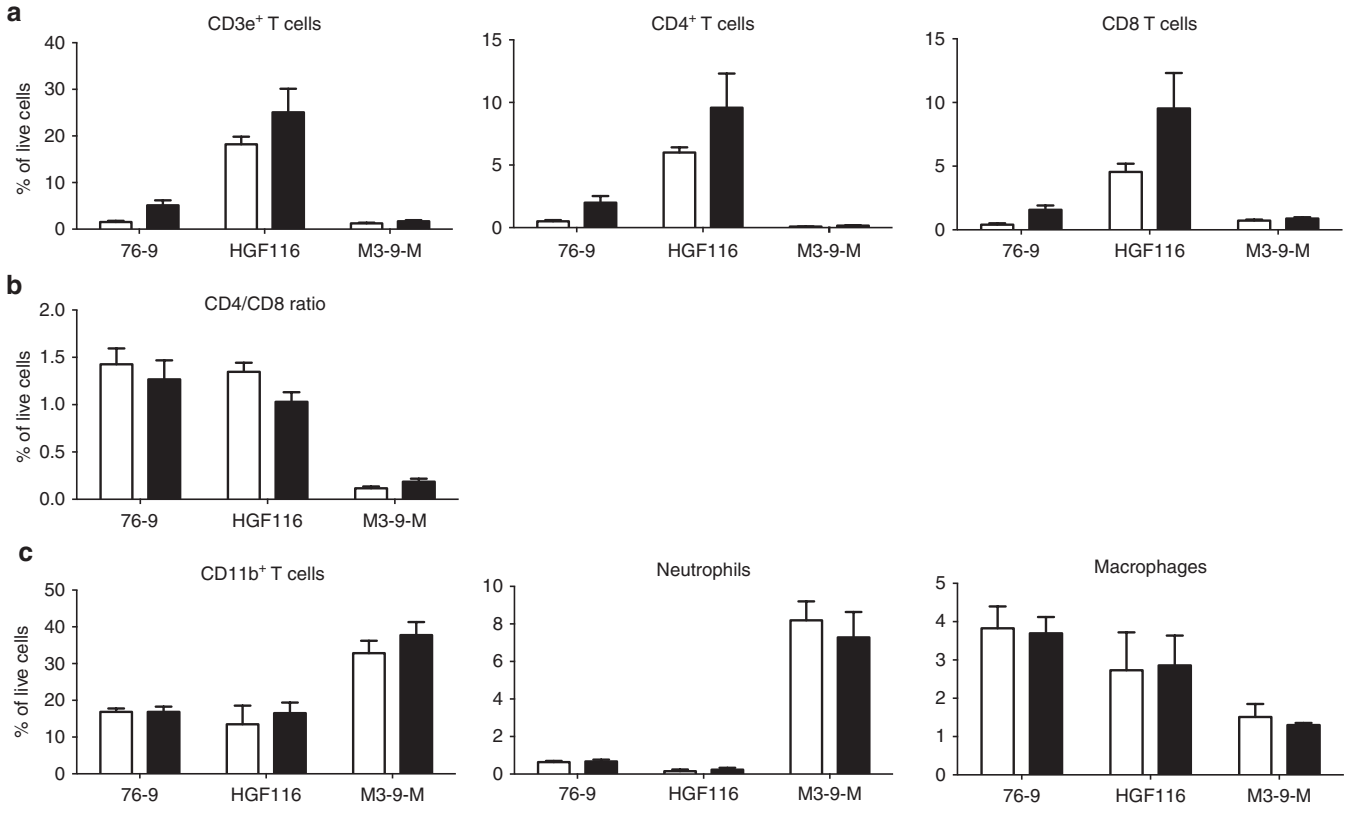

Figure 6 Mouse sarcoma models display baseline and virus-induced differences in tumor infiltrating lymphocyte and myeloid cell populations. Mouse sarcoma cell lines were implanted subcutaneously into the flanks of female C57Bl/6 mice. A single dose of PBS control or 1×10^8 pfu of rRp450 was delivered by fractionated intratumoral injection. Seven days postinfection, (**a,b**) tumor-infiltrating T-cell populations were analyzed by flow cytometry. (**c**) Tumor-associated myeloid cell populations were analyzed 72 hours postinfection. Error bars, SD ($n = 5$).

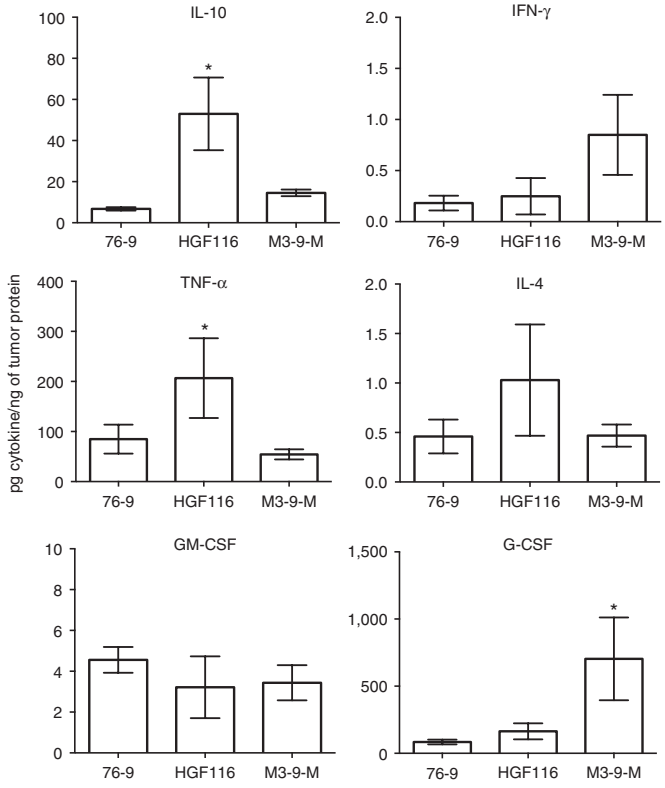

Figure 7 Mouse sarcoma models display baseline differences in the cytokine environment. Mouse sarcoma cell lines were implanted subcutaneously into the flanks of female C57Bl/6 mice. A single dose of 1×10^8 pfu of rRp450 or PBS control was delivered by fractionated intratumoral injection, and intratumoral cytokine levels were determined by milliplex analysis of homogenized tumor lysates. Baseline cytokine levels, normalized to total tumor protein, are shown for all PBS-treated time points pooled. Error bars, SD (n = 8–10).

Immune cell composition

As one potential explanation for lack of efficacy in HGF116, we hypothesized it may have a deficit in T-cell trafficking to the tumor. In fact, the virus-resistant tumor model HGF116 displayed the highest proportion of tumor-infiltrating T cells both at baseline and 7 days after a single injection of oHSV as measured by flow cytometry (Figure 6a), effectively ruling out a defect in T-cell trafficking. We observed no significant influx of myeloid populations 3 days following oHSV injection, though there were significant differences in the baseline myeloid composition of each tumor. The sensitive model M3-9-M displayed the highest baseline levels of neutrophils (Figure 6c), which have previously been reported to correlate with high endogenous IFN responsiveness[22] and contribute to oHSV antitumor efficacy through unknown mechanisms.[23] The resistant model HGF116 and intermediate responder 76-9 showed lower overall myeloid cells at baseline, which were dominated by tumor-associated macrophages.

Cytokine microenvironment

We also measured several immunomodulatory cytokines as a possible explanation for differences in antitumor efficacy (Figure 7). HGF116, the most resistant model, displayed significantly higher baseline levels of IL-10 and TNF-α. There was also a trend toward higher baseline IL-4 in this model, though it did not reach statistical significance. The most sensitive model, M3-9-M, displayed higher baseline concentrations of the immunostimulatory cytokine IFN-γ (P = 0.10; see Supplementary Figure S5, for time course.) We observed no differences in baseline or virus-induced intratumoral GM-CSF levels; however, M3-9-M did display significantly higher G-CSF.

DISCUSSION

We found that the therapeutic effect of oHSV in immunocompetent sarcoma models varied widely and was at least partially T-cell mediated. Interestingly, our analysis of the *in vitro* response to oHSV in these models revealed no correlation between the *in vivo* therapeutic effect and HSV-receptor expression, tumor cell susceptibility to oHSV infection, permissivity for viral replication, or sensitivity to oHSV-mediated oncolysis.

A similar requirement for a strong tumor antigen has been reported previously in a HER2/neu transgenic breast cancer model, where antigen naive mice demonstrated antitumor efficacy, with some tumor regression, while tolerized HER2/neu transgenic mice were resistant to the effects of oHSV.[24] Although these authors went on to demonstrate that antiviral CD8 T cells have the potential to kill bystander uninfected tumor cells in *in vitro* T-cell killing assays, the contribution of anti-HSV T cells to the overall therapeutic response in tolerized tumor models is unclear. Whether or not the modest antitumor effect we observed in M3-9-M male mice is T-cell mediated, either against viral antigens or subdominant tumor epitopes, remains to be determined. However, the similar pattern of tumor-growth delay observed in C57Bl/6 mice and athymic nude mice suggest that it could be T-cell independent. Altogether, these studies highlight the importance of tumor cell immunogenicity in determining the antitumor T-cell response to oHSV and raise the possibility that oHSV therapy is likely to be most effective in those tumors with strong tumor-specific antigens.

This striking disconnect between *in vitro* sensitivity and the *in vivo* therapeutic effect must be conveyed with the caveat that the lack of significant *in vivo* virus replication in these models suggests that direct tumor cell debulking through successive rounds of virus replication plays a minimal role in these immunocompetent RMS models. Although all three tumors were permissive to oHSV replication *in vitro*, there was minimal *in vivo* viral replication in any model. This finding is in stark contrast to many human xenograft models. For example, sensitive RMS tumor cell lines Rh30 and Rh41, used for *in vitro* comparison in this study, displayed nearly identical *in vitro* permissivity to oHSV replication as our murine models, yet they supported 3–4 logs of *in vivo* virus replication over the same time frame.[15,16] As *in vivo* virus replication in murine RMS models was also minimal in athymic nude mice, the observed difference in *in vivo* permissivity between mouse and human sarcoma tumors is likely tumor-cell intrinsic, rather than mouse strain specific. *In vitro* and *in vivo* analysis of mouse sarcomas revealed an intact IFN response pathway in all murine tumor models that may represent a major barrier to oHSV replication *in vivo*. Although exogenous type I IFN also inhibited virus replication in the human cell lines, the effect was species specific; thus, if the major source of type I IFN *in vivo* is host (stromal and/or immune cells), it would not have an effect in the xenograft models.

Given the lack of correlation with virus replication and antitumor activity, we further assessed the cellular and molecular tumor microenvironment of these three models. Analysis of tumor infiltrating lymphocytes revealed several interesting points. First, the lack of antitumor T-cell activity in the virus resistant model HGF116 is not due to a defect in T-cell trafficking to the tumor. In fact, HGF116 displayed the highest baseline and virus-induced infiltration of both CD4 and

CD8 T cells. However, the cytokine profile of this model, dominated by high expression of IL-10, is suggestive of an immunosuppressive microenvironment, unfavorable to induction of antitumor immunity. In contrast, the most sensitive model displayed higher IFN-γ and an increased ratio of cytotoxic CD8/CD4 T-cells following oHSV injection. We plan to test the role of these cytokines and cells on virotherapy using depletion strategies and knock-out mice in future experiments.

In conclusion, in three diverse models of pediatric sarcoma, we found that *in vitro* permissiveness for oHSV replication and sensitivity to oncolysis was not predictive of the *in vivo* therapeutic effect. Despite poor *in vivo* virus replication in all models, rRp450 was able to exert T-cell–mediated antitumor effects in two of three models, including robust tumor regression in a nontolerized model expressing the moderately immunogenic HY antigen. The precise mechanisms underlying sensitivity and resistance to oHSV therapy in these models are beyond the scope of this work but are likely linked to tumor cell immunogenicity and the quality of the immunologic microenvironment.

MATERIALS AND METHODS

Cell lines and viruses

Human RMS cancer cell lines RD (embryonal RMS) and Rh30 (alveolar RMS) were obtained from American Type Culture Collection (ATCC, Manassas, VA). Rh18 (eRMS) and Rh41 (aRMS) were obtained from the Pediatric Preclinical Testing Program (Peter Houghton, Nationwide Children's Hospital). All human RMS cell lines were maintained in RPMI supplemented with 10% fetal bovine serum (FBS), L-glutamine, and 100 IU/ml penicillin and 100 µg/ml streptomycin. Established mouse RMS tumor cell lines, 76-9 (methylchloranthrene-induced) and M3-9-M (*HGF/SF*$_{tg}$, *p53*$^{-/-}$) were kindly provided by Dr Brenda Weigel (University of Minnesota) and Dr Crystal Mackall (National Cancer Institute), respectively. HGF116 was derived from a spontaneous neck mass in a female *HGF/SF*$_{tg}$, *INK4a/Arf*$^{-/-}$ C57Bl/6 mouse. Mouse RMS cell lines were maintained in RPMI supplemented with 15% FBS, L-glutamine, nonessential amino acids, 2-mercaptoethanol, and 100 IU/ml penicillin and 100 µg/ml streptomycin. The *ICP6*-deficient oHSV vector rRp450 (KOS strain) was a kind gift of Dr Antonio Chiocco (Brigham and Women's Hospital, Boston, MA). The wild-type gD virus (K26GFP) and its receptor-restricted derivatives K26-gD:d5-28V (Nectin-1 restricted) and K26gD: A3C/Y38C (HVEM-restricted) were prepared as described in ref. 20. Other viral stocks were prepared with the 7b cell line[25] in 10-layer Nunc Cell Factories (Thermo Fisher Scientific, Waltham, MA) at a multiplicity of infection of 0.005 and purified under good laboratory practice–like conditions as previously described.[26] Titers were determined in triplicate on 7b cells according to standard protocols.[26]

Cell survival/MTS assay

2.5×10^3 RMS cells were plated in 96-well dishes and incubated at 37 °C overnight and then infected with oHSV mutant rRp450 at MOIs 0.001, 0.01, 0.1, 1, and 10 in sextuplicate. Cell viability was determined by CellTiter96 AQueous Non-Radioactive Cell Proliferation Assay (Promega, Madison, WI) according to manufacturer's instructions 4 days after virus infection. Data represented are percent cell survival relative to mock-infected controls.

In vitro virus replication assays

Mouse or human RMS cells were plated in 24-well dishes at 2×10^5 cells per well and then infected with 100 µl oncolytic HSV rRp450 at MOI 0.01. Following a 2-hour incubation with gentle shaking every 20 minutes, both cells and supernatants were harvested at 2, 24, 48, and 72 hours postinfection. Samples were freeze-thawed three times, diluted, and titered on Vero cells (ATCC) by standard plaque assay. For experiments addressing the effect of IFN on virus replication, mouse RMS cells were treated for 12 hours with 10–1,000 U of recombinant mouse IFN-β (PBL Assay Science, Piscataway, NJ) prior to infection with the oncolytic virus rRp450 at MOI 0.01, and total infectious virus was measured by standard plaque assay at the indicated times postinfection.

Animal studies

Animal studies were approved by the Institutional Animal Care and Use Committee at Cincinnati Children's Hospital and Nationwide Children's Hospital. To establish tumors, mouse RMS cell lines were suspended in PBS at 5×10^6 cells/100 µl and injected subcutaneously into the flanks of 5–6-week-old C57Bl/6 or athymic nude mice (Harlan Sprague Dawley, Indianapolis, IN). Tumor size was measured by caliper twice weekly and tumor volume calculated by the formula $V = L \times W^2 \times \pi/6$, where L is the length of the longest tumor axis and W is the width of the longest approximately perpendicular axis. When tumors reached 100–300 mm^3, rRp450 or PBS control was delivered by fractionated intratumoral injection to achieve widespread virus distribution, as we have previously reported.[16] For survival studies, 1×10^8 pfu of rRp450 or PBS control was delivered on days 0, 2, and 4. For analysis of *in vivo* virus replication, a single unfractionated dose of 1×10^7 rRp450 was injected into established tumors, and mice were sacrificed for tumor dissection 2, 24, 72, and 120 hours postinjection. Tumors were dissected, homogenized using a hand-held tissue homogenizer, and subjected to three freeze/thaw cycles prior to assaying viral titer by standard plaque assay on Vero cells.

RNA extraction

Total RNA was isolated from 1×10^6 cells or an appropriate weight of mechanically pulverized tumor powder using the RNeasy Plus Mini Kit (Qiagen, Valencia, CA) per manufacturer's instructions. The concentration and purity of the recovered RNA was determined measuring the optical density at 260 and 280 nm.

Quantitative RT-PCR

Five micrograms of total RNA was used to generate cDNA with SuperScript II Reverse Transcriptase (Life Technologies, Carlsbad, CA) per the manufacturer's instruction. Quantitative real-time PCR was then performed using the Applied Biosystems 7900 (Waltham, MA). Cycling conditions were 10 minute denaturation at 95 °C, 40 successive cycles of 94 °C for 15 seconds, 58 °C for 30 seconds, and 72 °C for 30 seconds, and a final incubation for 5 minutes at 72 °C. Comparative quantitative method was used for data analysis. Data are represented as fold gene expression relative to *glyceraldehyde 3-phosphate dehydrogenase*. The primers used in this study are listed in Supplementary Table S1.

Viral gene transfer assays

RMS cells were seeded at a density of 2×10^5 cells per well in a 12-well dish, incubated overnight, and then infected with 20–200 genome copies per well with GFP-expressing wild-type gD virus (K26GFP) and its receptor restricted derivatives K26-gD:d5-28V (Nectin-1 restricted) and K26gD: A3C/Y38C (HVEM-restricted). Twenty-four hours postinfection, cells were washed with PBS to remove unbound virus and with acidic glycine buffer (pH 3.0) to remove external cell-associated virus. Cells were harvested and prepared for flow cytometric analysis.

Flow cytometry for HSV receptor expression

Human RMS tumor cell lines were harvested by nonenzymatic cell dissociation buffer and passed through a 70 µm cell strainer to obtain a single cell suspension. Approximately 1×10^6 tumor cells were resuspended in 100 µl buffer (PBS, 1% FBS, 1% ethylenediaminetetraacetic acid) and blocked with 20% final volume Ig Fc blocking antibody for the appropriate species, either human Fc block (Miltyni Biotech, San Diego, CA) or mouse Fc block (BD biosciences, San Jose, CA). Blocked cell suspensions were stained with 1:100 dilutions of HSV receptor antibodies to Nectin-1 (R1.302.12. sc-6918), Nectin-2 (R2.525 sc-32804), and HVEM (CW10 sc-21718), or mouse IgG isotype control (sc-3878) (Santa Cruz Biotechnology, Santa Cruz, CA) for 20 minutes at room temperature. Following primary stain, samples were washed with 1 ml buffer and stained with fluorescein isothiocyanate–conjugated goat antimouse IgG (Southern Biotech, Birmingham, AL). Following two washes, cells were fixed in 1% paraformaldehyde and analyzed on a BD FACSCanto II using FlowJo version 9.4.10 (Tree Star, Ashland, OR).

Flow cytometry for cellular influx

Tumor single cell suspensions were obtained by mechanical chopping and incubation in 25 µg/ml liberase blendzyme 3 (Roche Life Sciences, Indianapolis, IN) and 250 µg/ml DNAse I for 1 hour at 37 °C. Tumor slurries were passed over a 70 µm cell strainer, washed in buffer (PBS, 1% FBS, and 1% ethylenediaminetetraacetic acid) and resuspended at ~2×10^6 cells/100 µl buffer containing 5% mouse Fc blocking reagent. For analysis of the innate and adaptive immune infiltrate, samples were stained with the following

antibodies CD11b (M1/70), F4/80 (BM8), GR1 (RB6-8C5), CD4 (GK1.5), CD8a (53-6.7), CD3e (145-2C11), NK1.1 (PK136) (Biolegend, San Diego, CA), and CD11c (N418) (eBiosciences, San Diego, CA). Samples were stained for 25 minutes on ice, followed by two washes with buffer. Cells were fixed in 1% paraformaldehyde and analyzed on a BD FACSCanto II as above. The gating strategy for identification and quantification of various cellular subsets is shown in Supplementary Figure S6.

Milliplex cytokine array

Frozen tumor tissue was mechanically pulverized and weighed. To standardize cytokine analysis between samples, the tissue was resuspended in 5 µl PBS containing 10 µl/ml protease inhibitor cocktail (Sigma P8340, St. Louis, MO: AEBSF, 1.04 mmol/l; Aprotinin, 0.80 µmol/l; Bestatin, 4.00 µmol/l; E-64, 14 µmol/l; Leupeptin, 2.00 µmol/l; and Pepstatin A, 15 µmol/l) per mg tissue weight and agitated at 4 °C for 1 hour. The samples were then centrifuged at 10,000 rpm for 5 minutes to collect supernatants. Supernatants were subjected to Bioplex analysis (BioRad, Hercules, CA) for the presence of cytokines as per manufacturer's instructions. Standard curve ranges: IL-2 (45,844.7 – 3.3 pg/ml), IL-4 (31,437.5 – 7.7 pg/ml), IL-10 (24,026.3 – 1.17 pg/ml), G-CSF (54,190.1 – 4.3 pg/ml), GM-CSF (12,357.1 – 9.8 pg/ml), IFN-γ (4,671.6 – 1.0 pg/ml), and TNF-α (44,691.2 – 2.6 pg/ml). Final observed cytokine concentration in pg/ml was divided by gram tissue weight for final pg/ml per gram tumor tissue.

Exogenous Nectin-1 expression

Construction of the human Nectin-1 expressing murine stem cell virus plasmid pMIEG3-hNectin-1 and retrovirus production were performed as previously described.[21] For retroviral transduction, 1×10^6 HGF116 cells were infected with a 50:50 mix of mouse sarcoma culture medium/viral supernatant plus 4 µg/ml polybrene. After incubation at 37 °C overnight, the supernatants were replaced with fresh culture medium. At 7 days posttransduction, EGFP-positive cells were FACS sorted, and cell-surface expression of human-Nectin-1 was confirmed via flow cytometry analysis.

ACKNOWLEDGMENTS

We thank Brian Geier for analysis of the Pediatric Preclinical Testing Program gene expression database, E. Antonio Chiocca (Brigham and Women's Hospital) for rRp450, and Crystal Mackall (National Cancer Institute), Brenda Wiegel (University of Minnesota), and Peter Houghton (Nationwide Children's Hospital) for cell lines. We thank Brooke Nartker for technical assistance. This work was funded in part by the Joanne Macafee Childhood Cancer Foundation, Cancer Free Kids Pediatric Cancer Research Alliance, The Katie Linz Foundation, and Nationwide Children's Hospital Research Institute.

REFERENCES

1 Ward, E, DeSantis, C, Robbins, A, Kohler, B and Jemal, A (2014). Childhood and adolescent cancer statistics, 2014 *CA Cancer J Clin* **64**: 83–103.
2 Smith, MA, Seibel, NL, Altekruse, SF, Ries, LA, Melbert, DL, O'Leary, M *et al*. (2010). Outcomes for children and adolescents with cancer: challenges for the twenty-first century. *J Clin Oncol* **28**: 2625–2634.
3 Kaur, B, Chiocca, EA and Cripe, TP (2012). Oncolytic HSV-1 virotherapy: clinical experience and opportunities for progress. *Curr Pharm Biotechnol* **13**: 1842–1851.
4 Hammill, AM, Conner, J and Cripe, TP (2010). Oncolytic virotherapy reaches adolescence. *Pediatr Blood Cancer* **55**: 1253–1263.
5 Kaur, B, Cripe, TP and Chiocca, EA (2009). "Buy one get one free": armed viruses for the treatment of cancer cells and their microenvironment. *Curr Gene Ther* **9**: 341–355.
6 Varghese, S and Rabkin, SD (2002). Oncolytic herpes simplex virus vectors for cancer virotherapy. *Cancer Gene Ther* **9**: 967–978.
7 (2002). Oncolytics Biotech releases REOLYSIN phase I clinical trial results. *Expert Rev Anticancer Ther* **2**: 139.
8 Rampling, R, Cruickshank, G, Papanastassiou, V, Nicoll, J, Hadley, D, Brennan, D *et al*. (2000). Toxicity evaluation of replication-competent herpes simplex virus (ICP 34.5 null mutant 1716) in patients with recurrent malignant glioma. *Gene Ther* **7**: 859–866.
9 MacKie, RM, Stewart, B and Brown, SM (2001). Intralesional injection of herpes simplex virus 1716 in metastatic melanoma. *Lancet* **357**: 525–526.
10 Fong, Y, Kemeny, N, Jarnagin, W, Stanziale, S, Guilfoyle, B, Gusani, N *et al*. (2002). Phase 1 study of a replication-competent herpes simplex oncolytic virus for treatment of hepatic colorectal metastases. *Proc Am Soc Clin Oncol* **21**: 8a, abstract #27.
11 Sheridan, C (2013). Amgen announces oncolytic virus shrinks tumors. *Nat Biotechnol* **31**: 471–472.
12 Kaufman, HL, Kim, DW, DeRaffele, G, Mitcham, J, Coffin, RS and Kim-Schulze, S (2010). Local and distant immunity induced by intralesional vaccination with an oncolytic herpes virus encoding GM-CSF in patients with stage IIIc and IV melanoma. *Ann Surg Oncol* **17**: 718–730.
13 Thorne, SH and Kirn, DH (2004). Future directions for the field of oncolytic virotherapy: a perspective on the use of vaccinia virus. *Expert Opin Biol Ther* **4**: 1307–1321.
14 Zanola, A, Rossi, S, Faggi, F, Monti, E and Fanzani, A (2012). Rhabdomyosarcomas: an overview on the experimental animal models. *J Cell Mol Med* **16**: 1377–1391.
15 Currier, MA, Gillespie, RA, Sawtell, NM, Mahller, YY, Stroup, G, Collins, MH *et al*. (2008). Efficacy and safety of the oncolytic herpes simplex virus rRp450 alone and combined with cyclophosphamide. *Mol Ther* **16**: 879–885.
16 Currier, MA, Adams, LC, Mahller, YY and Cripe, TP (2005). Widespread intratumoral virus distribution with fractionated injection enables local control of large human rhabdomyosarcoma xenografts by oncolytic herpes simplex viruses. *Cancer Gene Ther* **12**: 407–416.
17 Meadors, JL, Cui, Y, Chen, QR, Song, YK, Khan, J, Merlino, G *et al*. (2011). Murine rhabdomyosarcoma is immunogenic and responsive to T-cell-based immunotherapy. *Pediatr Blood Cancer* **57**: 921–929.
18 Weigel, BJ, Rodeberg, DA, Krieg, AM and Blazar, BR (2003). CpG oligodeoxynucleotides potentiate the antitumor effects of chemotherapy or tumor resection in an orthotopic murine model of rhabdomyosarcoma. *Clin Cancer Res* **9**: 3105–3114.
19 Sharp, R, Recio, JA, Jhappan, C, Otsuka, T, Liu, S, Yu, Y *et al*. (2002). Synergism between INK4a/ARF inactivation and aberrant HGF/SF signaling in rhabdomyosarcomagenesis. *Nat Med* **8**: 1276–1280.
20 Uchida, H, Shah, WA, Ozuer, A, Frampton, AR Jr, Goins, WF, Grandi, P *et al*. (2009). Generation of herpesvirus entry mediator (HVEM)-restricted herpes simplex virus type 1 mutant viruses: resistance of HVEM-expressing cells and identification of mutations that rescue nectin-1 recognition. *J Virol* **83**: 2951–2961.
21 Wang, PY, Currier, MA, Hansford, L, Kaplan, D, Chiocca, EA, Uchida, H *et al*. (2013). Expression of HSV-1 receptors in EBV-associated lymphoproliferative disease determines susceptibility to oncolytic HSV. *Gene Ther* **20**: 761–769.
22 Fu, X, Tao, L, Rivera, A, Xu, H and Zhang, X (2011). Virotherapy induces massive infiltration of neutrophils in a subset of tumors defined by a strong endogenous interferon response activity. *Cancer Gene Ther* **18**: 785–794.
23 Workenhe, ST, Pol, JG, Lichty, BD, Cummings, DT and Mossman, KL (2013). Combining oncolytic HSV-1 with immunogenic cell death-inducing drug mitoxantrone breaks cancer immune tolerance and improves therapeutic efficacy. *Cancer Immunol Res* **1**: 309–319.
24 Sobol, PT, Boudreau, JE, Stephenson, K, Wan, Y, Lichty, BD and Mossman, KL (2011). Adaptive antiviral immunity is a determinant of the therapeutic success of oncolytic virotherapy. *Mol Ther* **19**: 335–344.
25 Krisky, DM, Wolfe, D, Goins, WF, Marconi, PC, Ramakrishnan, R, Mata, M *et al*. (1998). Deletion of multiple immediate-early genes from herpes simplex virus reduces cytotoxicity and permits long-term gene expression in neurons. *Gene Ther* **5**: 1593–1603.
26 Goins, WF, Huang, S, Cohen, JB and Glorioso, JC (2014). Engineering HSV-1 vectors for gene therapy. *Methods Mol Biol* **1144**: 63–79.

Supplementary Information accompanies this paper on the *Molecular Therapy—Oncolytics* website (http://www.nature.com/mto)